

# Unit-cell driven deterministic inverse design of metasurface antennas

Leonardo Pollini, Marcello Zucchi, and Giuseppe Vecchi

Department of Electronics and Telecommunications, Politecnico di Torino, Turin, Italy

**Abstract**—This contribution presents a metasurface (MTS) design carried on with a current-only optimization approach. The standard MTS optimization in literature treats the impedance profile as continuous, with subsequent sampling at the center of unit cells. Here, optimization is carried out dividing the MTS surface into isolated subdomains that correspond to the intended unit cells, which will make the final unit cell designed easier. This is compared to the case in which the impedance profile is treated as continuous; results show that the synthesized impedance profile and the resulting radiation pattern are comparable, thus paving the way to a better design of the overall MTS.

## I. INTRODUCTION

The design of metasurfaces (MTS) has received continuous attention in recent years because of the importance of these structures. Virtually all design approaches for large size MTS employ the homogenization of sub-wavelength features into the Impedance Boundary Conditions (IBC); this allows separating the design of the impedance profile from the final step of realizing it with unit cells: this will also be the underlying approximation in this communication. The design of the impedance profile has been approached in two ways: a) global optimization, with parametric profiles with few degrees of freedom; and b) current-only approaches [1]–[7]. In the latter, only the equivalent current is the direct object of the design, and the impedance profile is obtained afterward as a post-processing: these methods have the advantage of a much lower numerical cost per-iteration, which allows a much higher flexibility in the obtainable impedance profiles.

Current-only approaches, on the other hand require enforcing that the current corresponds to a passive and lossless structure: this is done either in a semi-analytical manner whenever a surface wave can be physically relevant [1], [2], or by direct enforcement in the optimization scheme [4], [5], [7]. In this study we employ a current-only approach of the latter sub-class.

All cited works assume the (equivalent) current flowing across the entire surface. In this contribution instead, we propose and test a different strategy, akin to the 1D approach in [6]: we perform the optimization subdividing the MTS in subdomains of dimensions corresponding to the final cells that are to be designed, and each subdomain is electrically isolated from its neighbors. Because of our focus, we will employ the approach in [5], as it allows a full 2D variability and freedom in the geometrical description.

## II. METASURFACE DESIGN APPROACH

The metasurface macroscopic behavior is simulated by employing thin layer of transparent (penetrable) surface

impedance over a dielectric grounded substrate [8]; we consider here a scalar Impedance Boundary Condition (IBC),

$$\mathbf{E}_{\text{tan}} = Z \hat{\mathbf{n}} \times (\mathbf{H}^+ - \mathbf{H}^-) = Z \mathbf{J}, \quad (1)$$

where  $Z$  denotes the local impedance value and  $\mathbf{J}$  represents the equivalent surface electric current. The problem is formulated as an integral equation (EFIE-IBC), as

$$\mathbf{E}_{\text{inc}} + \mathcal{L}\mathbf{J} = Z\mathbf{J}, \quad (2)$$

where  $\mathbf{E}_{\text{inc}}$  represents the source field and the operator  $\mathcal{L}$  is the Electric Field Integral Operator (EFIO). The equation is discretized via standard Method of Moments; we use a triangular mesh and the current is expanded as a linear combination of Rao-Wilton-Glisson (RWG) basis functions. The optimization problem is then formulated as the unconstrained optimization of a non-convex objective function that takes into account both *realizability* and *radiation* constraints expressed only in terms of the current coefficients. The minimization is performed with a non-linear conjugate gradient algorithm that provides the optimized current  $\mathbf{J}^*$ .

As stated above, we will consider isolated subdomains in the optimization, as exemplified in Fig. 1b. This approach is expected to have two advantages: a) the impedance profile is closer to the actual antenna to be realized with unit cells; b) the size of the optimization space is significantly smaller (we recall that all mesh edges are optimization parameters).

The impedance profile is computed from the optimized current. While the impedance reconstruction of the continuous case depends on the current value of the single triangle, in the other case, all triangles inside a unit cell are associated with the same impedance value. This quantity is obtained extending the treatment in [5], minimizing the squared error within the EFIE-IBC equation (2) over each specific unit cell domain  $\mathcal{S}_i$  with closed-form solution given by

$$Z_i = \frac{\langle \mathbf{E}_{\text{tan}}^*, (\mathbf{J}^*)^* \rangle_{\mathcal{S}_i}}{\|\mathbf{J}^*\|_{\mathcal{S}_i}^2}, \quad (3)$$

## III. APPLICATION EXAMPLES

The case of study consists in a circular metasurface antenna with a diameter  $d = 78.2 \text{ mm} \approx 6\lambda$  ( $\lambda = c/f$ ), designed at a frequency of 23 GHz over a grounded dielectric with  $\epsilon_r = 3.34$  and thickness  $h = 0.508 \text{ mm}$ . The antenna is excited by a cylindrical  $\text{TM}_0$  surface wave. The radiation constraints consist in a linearly polarized pencil beam radiation pattern,

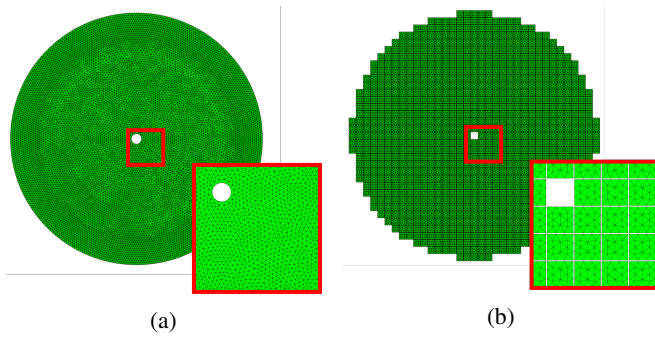


Fig. 1: Overall antenna discretization; (a) continuous domain, (b) square cells partitioning with  $100\mu\text{m}$  between the cells. The insets show the underlying mesh employed.

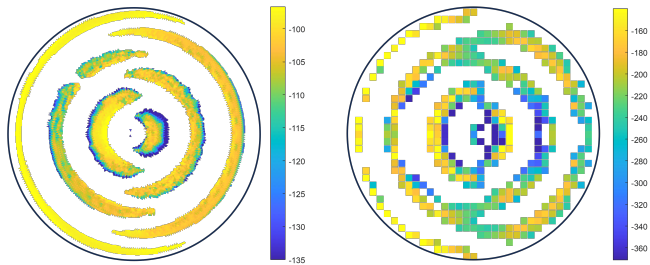


Fig. 2: Synthesized imaginary part of impedance profile for: (a) continuous geometry and (b) square cells geometry. White areas mean open circuit (absence of impedance).

with gain maximization in the broadside direction and side-lobes level below  $-20$  dB; the actual target is  $-15$  dB, but we expect some loss of efficiency in impedance computation. The impedance was constrained to be capacitive, with reactance in the range between  $-100$  and  $-800$  Ohm, coherent with the substrate, frequency and cell size (see below).

Two geometries have been considered:

- 1) Continuous domain, Fig.1a;
- 2) Square cell partitioned: cell size of  $\lambda/6$  separated by  $100\mu\text{m}$  gaps, Fig.1b.

in both cases, the average mesh size is  $\lambda/18$ . The patterns have been obtained starting from the optimized current as follows: a) impedance profile recovery from current (Figs. 2), b) EFIE-IBC simulation of the obtained impedance profiles; hence, all results include possible loss of efficiency in impedance retrieval. In the verification step (b), for cell partitioning (2) the impedance was constant over each cell.

#### IV. CONCLUSIONS

We have discussed a MTS design approach using a cell-level partitioning of the geometry with a realizable gap; we have shown that the performance are equivalent to or better than the continuous approach, while simplifying final design.

#### ACKNOWLEDGEMENT

This work was supported by the European Union's Horizon 2020 research and innovation programme under the Marie

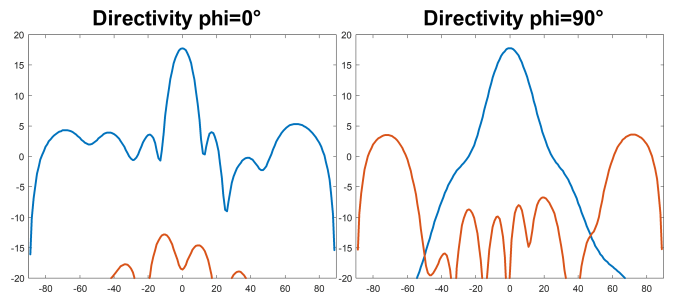


Fig. 3: Directivity pattern for the continuous geometry; left: E plane, right: H plane

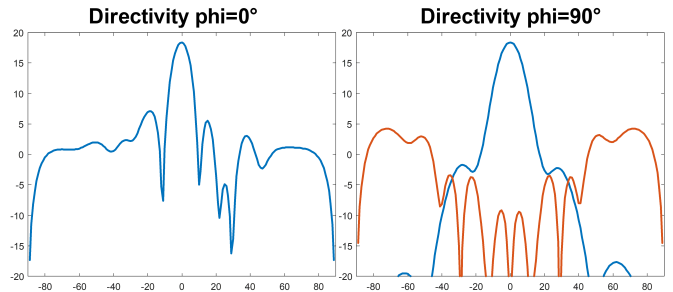


Fig. 4: Directivity pattern for separated square cells geometry (cross polar below scale bottom where not show). Left: E plane, right: H plane

Skłodowska-Curie grant agreement No 955476.

#### REFERENCES

- [1] G. V. E. A. Epstein, "Synthesis of passive lossless metasurfaces using auxiliary fields for reflectionless beam splitting and perfect reflection," *Phys. Rev. Lett.*, 2016.
- [2] M. Bodehou, C. Craeye, E. Martini, and I. Huynen, "A Quasi-Direct Method for the Surface Impedance Design of Modulated Metasurface Antennas," *IEEE Transactions on Antennas and Propagation*, vol. 67, no. 1, pp. 24–36, Jan. 2019.
- [3] T. Brown, C. Narendra, Y. Vahabzadeh, C. Caloz, and P. Mojabi, "On the Use of Electromagnetic Inversion for Metasurface Design," *IEEE Transactions on Antennas and Propagation*, vol. 68, no. 3, pp. 1812–1824, Mar. 2020.
- [4] T. Brown and P. Mojabi, "Cascaded Metasurface Design Using Electromagnetic Inversion With Gradient-Based Optimization," *IEEE Transactions on Antennas and Propagation*, vol. 70, no. 3, pp. 2033–2045, Mar. 2022.
- [5] C. C. P. M. T. Brown, Y. Vahabzadeh, "Electromagnetic inversion with local power conservation for metasurface design," *IEEE Antennas Wireless Propag. Lett.*, 2020.
- [6] J. Budhu and A. Grbic, "Perfectly Reflecting Metasurface Reflectarrays: Mutual Coupling Modeling Between Unique Elements Through Homogenization," *IEEE Transactions on Antennas and Propagation*, vol. 69, no. 1, pp. 122–134, Jan. 2021.
- [7] M. Zucchi, F. Verni, M. Righero, and G. Vecchi, "Current-Based Automated Design of Realizable Metasurface Antennas with Arbitrary Pattern Constraints," *IEEE Transactions on Antennas and Propagation*, 2023.
- [8] M. A. Francavilla, E. Martini, S. Maci, and G. Vecchi, "On the Numerical Simulation of Metasurfaces With Impedance Boundary Condition Integral Equations," *IEEE Transactions on Antennas and Propagation*, vol. 63, no. 5, pp. 2153–2161, May 2015.